British Journal of Applied Science & Technology
5(2): 173-188, 2015, Article no.BJAST.2015.017
ISSN: 2231-0843

SCIENCEDOMAIN *international*
www.sciencedomain.org

Design and Evaluation of a Dissolved Oxygen Controller for Solar Powered Fish Tanks

Federico Hahn[1*] and Ruth Pérez[2]

[1]IAUIA, Department of Agricultural Engineering and Water Use, Chapingo Autonomous University, Texcoco, México.
[2]TEBIINS, Department of R&D, San Mateo Huexotla, Mexico.

Authors' contributions

This work was carried out in collaboration between both authors. Author FH designed the controller, installed the photovoltaic equipment, performed the tests and wrote the first draft of the manuscript. Author RP analyzed the cloud sensor measurements, acquired data from the weather station and developed literature searches. Both authors read and approved the final manuscript.

Article Information

DOI: 10.9734/BJAST/2015/13034
Editor(s):
(1) Ahmed Mohamed El-Waziry, King Saud University, College of Food and Agriculture Sciences, Kingdom of Saudi Arabia.
Reviewers:
(1) Apolinar Santamaría Miranda, Departamento de Acuacultura, CIIDIR-IPN Unidad Sinaloa, Guasave, México.
(2) Anonymous, Tokyo University of Marine Sciences and Technology, Japan.
(3) Nnaji Chibueze Eze, National Centre for Energy Research and Development, University of Nigeria, Nsukka, Nigeria.
(4) Anonymous, Federal University of Goiás, Brazil.
Complete Peer review History: http://www.sciencedomain.org/review-history.php?iid=713&id=5&aid=6579

Original Research Article

Received 30th July 2014
Accepted 29th August 2014
Published 22nd October 2014

ABSTRACT

Aims: A dissolved oxygen controller was designed to optimize photovoltaic energy and maintain minimum DO variations in the fish tanks, independent on environmental conditions.
Study Design: Software critical parameters have to be tuned including discontinuous routine (DR) interval, use throughout the night and cloud sensing.
Place and Duration of Study: Department of Irrigation at Tlapeaxco, Texcoco, Mexico at the Universidad Autonoma Chapingo, between April and July 2011.
Methodology: The controller was assembled and its software tested to maintain the desired water dissolved oxygen concentration in the tanks. Solar radiation and clouds presented during May and June of 2011 were monitored correlating an infrared sensor with a sunshine indicator. Energy produced by the solar panels was acquired with a data logger together with the energy stored in the batteries; overvoltage and deep discharges were avoided by the battery. A discontinuous routine was turned on when clouds were present, evaluating whether it should operate during all the night.

**Corresponding author: E-mail: fedhahn@gmail.com;*

Results: May presented 26 cloudy days and 45% of these days presented less than 2 hours of more than 1000 W/m^2 of irradiation. Cloud cover sensing correlation between the infrared and sunshine sensor has a R^2=0.97. Cloud cover peaks can last from minutes to hours and using the one-hour discontinuous routine (DR) instantaneous peaks were avoided. Optimal DR period was ten minutes as it saves the same quantity of energy but maintains dissolved oxygen (DO) concentration over 4.1 ppm; hourly DR intervals, decreases DO to 2.4 ppm stressing the carps. Battery charge should be at least 39 Ah@19:00 to supply the energy required by the aerators during the night.
Conclusion: A sunshine sensor was selected to detect cloud cover and its sampling period was decreased from ten to one minute. DO concentration on tanks became more stable when the ten minute discontinuous period was employed.

Keywords: Cloud sensor; DO controller; photovoltaic driven aerators; energy management; night aeration; discontinuous aeration application.

1. INTRODUCTION

Automation of aquaculture systems improves environmental control by minimizing effluents, reducing production costs and improving product quality. At high production densities, a failure in a circulation pump or aeration system can put fish under severe stress or cause significant losses within minutes [1]. Lethal effects should be avoided by monitoring the most highly oxygenated sections where fish go [2]. Automated aerator activation reduces energy and night labor crew expenses to a minimum; low concentration of dissolved oxygen (DO) limits fish growth and production in intensive aquaculture. DO in recirculating systems should be monitored closely, before and after feedings [3]. However, dissolved oxygen *in situ* measurements are difficult to monitor over long periods of time. When flow rates, water depth, turbidity and/or weather conditions fluctuate DO variations are difficult to predict.

Aeration blowers and water pumping are the main energy consuming equipment in aquaculture at the farm level and electricity accounts for 29% of tilapia production cost [4]. Usually aeration is supplied 24 h per day for at least 100 days for the production of marine shrimp in ponds [5]. Aerators mechanically or electrically driven increase dissolved oxygen in water; aeration is the process of bringing water and air into close contact. Various types of aeration can be found in the field, ranging from splasher system, paddlewheel, bubbler and pump [6]. In Asia, paddlewheel aerators often are driven by small internal combustion engines [5] or by photovoltaic cells [7].

Several embedded systems have been developed to monitor and control dissolved oxygen in aquaculture. A PIC 18F4550 microcontroller was developed to control water and air pumps using relays in n aquaponic system [8]. A PIC 16F877A microcontroller controlled the aeration of tanks [9] based on a decision support system (DSS) for fish farm planning on ponds. An ATmega16 connected with ZigBee modules monitored pH, DO, temperature and water level in real time at the Tanggu fish pond [10]; data were introduced to a computer and processed with LabVIEW software, sending short messages to the producers via GSM.

Photovoltaic systems are being used in places with high solar irradiation and where electricity is not available. Knowledge of the local solar-radiation is essential for the proper design of solar energy systems [11]; Sunshine hours and cloud-cover were obtained from many meteorological stations. Seven models using the Ångström-Prescott equation predicted the average daily global radiation with hours of sunshine [12]. A PV floating power generation system consisting of a floating system and a PV system with underwater cables presented 10.3% more energy production than an overland PV system [13]. A wind-solar complementary system was developed increasing oxygen content in water, saving power, reducing aquaculture costs and increasing aquaculture production [14].

In this paper a DO controller system was designed monitoring DO in four fish tanks. The entire RAS (recirculated aquaculture system) is powered by a solar system, so after checking the cloud cover and the battery it decides whether to turn-on the aerators continuously, discontinuously oreven using a diesel generator. Requirements for controller software were encountered considering discontinuous

oxygenation period, night operation and cloud detection sampling.

2. MATERIALS AND METHODS

The aquaculture recirculation system (RAS) is located at Tlapeaxco, Chapingo, Mexico at the experimental facilities of the Universidad Autonoma Chapingo. The system installed within a greenhouse is comprised of 4 independent RAS (recirculation aquaculture system). An ATmega16L microcontroller was used to monitor and control dissolved oxygen in four culture tanks. The controller (Fig. 1, J) was designed to:

- Monitor DO at each tank;
- Turn-on aerators remotely;
- Detect cloud presence;
- Data logging of DO data.

2.1 Recirculation Aquaculture System Prototype

Each RAS is comprised of a culture tank (Fig. 1, A), solid waste separator, two column aerator and a bio-filter. The water from each circular polyethylene culture tank (1.1 m diameter and 1100 L capacity) circulated through the solid waste separator before entering into a trickling bio-filter with polyethylene bio-strata, (Fig. 1, D). The solid waste separator (Fig. 1, B) was developed combining a swirl separator and a radial flow settler in order to maximize the sedimentation efficiency. The spray column aerator is fed from the bio-filter through a 90 W@120 AC pump (mod DB5, Finish Thompson Inc., USA), (Fig. 1, F). The water coming out from the bio-filter is recirculated to the culture tank by means of a 90 W@120 AC pump (mod DB3, Finish Thompson Inc., USA) which provides 40 L/min at a pressure of one meter, (Fig. 1, G).

The spray column aerator (Fig. 1, C) consists of plastic shells having a volume of 0.4276m^3 (0.55m diameter x 1.80 m height) with two mass transfer units (each 0.9m long). The two units were separated by a water distributor plate having 65 holes (diameter 0.02 m) to allow that air and water passes through it. As water flows through the top of the spray tower, three fine conical jet sprays (mod. 130327, SURTEK, MEX) increase water oxygenation. The aerator (Fig. 1, E) uses a 1/2 HP AC motor, integrated to a recirculating water pump to lift the water to the spray column aerator, (Table 1); both are controlled by a solid state switch found at the embedded control board. If the recirculation pump is turned off with the aerator on, the bio-filter gets oxygenated. When culture tank is recirculated and aeration turned-off, water is provided by the bio-filter.

The four tanks were stocked at two different times with mirror carp var. *Cyprinus carpio*, which were harvested every 37 days; harvest size was 400 g after 5 months of cultivation. Stocking density per tank was 50 fish weighing 25 kg per m^3. The first and second tanks were stocked in December 2011, meanwhile the third and fourth in February 2011. Carps were fed with a commercial fish food recommended for rearing tanks (Nutripec 3508) at 9:00, 14:00 and 19:00 hr. These floating pellets have a diameter of 3.5 mm, 35% protein, 8% fat and an apparent density of 415 kg/m^3. Fish were necessary during the experiment to consume oxygen and test the controller but no fish growth studies are reported here.

2.2 Photovoltaic System

The photovoltaic system (PV) supplies the energy to recirculate and oxygenate the water within the RAS system, (Fig. 1, H). The energy harvested by the solar panels is supplied to the RAS system and the remaining energy stored in batteries; an inverter converts DC to AC voltage [15]. Solar irradiance (H) in the 0-1250 W/m^2 was measured with a silicon pyrometer (mod S-LIB-M003, HOBO, USA) every minute. The values acquired during the daylight were exported to an Excel file and the current generated in A(I_{sp}) every minute by the panel was obtained from Eqn.1. A data-logger (mod LabPro, Vernier, USA) measured the current in amperes supplied to the aquaculture system every minute, I_{ras}. The current stored in the battery (I_B) in A was obtained with Eqn. 2.

$$I_{sp} = H/123.71 \quad (1)$$

$$I_B = I_{sp} - I_{ras} \quad (2)$$

Solar irradiance was obtained daily from an automated meteorological station (Davis_Instruments-Vantage Pro) located at Montecillo, Texcoco at latitude 19° 27' 38" N and longitude 98° 54' 01" W. Two months of daily data helped to analyze the effect of the clouds in the solar radiation, its effect in solar panel energy generation and cloud detection by the DO controller.

Solar panel and batteries were selected to provide continuous energy provision considering four hours of irradiance above 1000 Wm^2/day [16]. Daily power consumption by one RAS and by the controller system was 92.6 Ah (AC voltage) and 56.1 Ah (DC voltage), respectively, (Table 1). If a 20% of additional charge is considered together with a battery efficiency of 85%, the energy required for the operation and monitoring of one RAS system is of 209.92 Ah. Four solar panels of 200 W each (mod. ES-A-205-fa2, Evergreen Solar, USA) were selected to provide 3 day of autonomy [15]. A bank of four 12 V@200 Ah rechargeable LiFePO4 batteries (Model SB-200, Smart Battery LLC, USA) was used together with a current battery charger. Ion lithium batteries are lighter and non-explosive; present a longer life with 3000 to 5000 life cycles and an automatic built in battery protection system. A 600 W, 12V DC - 120V AC inverter (mod SA-600R, Samlex, USA) was selected to provide AC energy to the aeratorextractors and re-circulating pumps.

2.3 Controller Design

The controller block diagram presents a microcontroller ATmega 16, a cloud detector together with incoming signals from the batteries and sensors, (Fig. 2). The controller was used to monitor and control dissolved oxygen in the four culture tanks using four optical dissolved oxygen sensors (ST 6115, B&C Electronics Srl, Milan, Italy) with automatic temperature compensation based on fluorescent technology. Each probe has a built-in 2-wire 4/20 mA transmitter with a 10 m cable; the signal is transformed to a 1-5 V signal by a 250Ω resistance. The probe measures DO in the 0 and 20 ppm range with a ±0.1 ppm O2 resolution, responds in 60 seconds and operates at temperatures ranging between 5 and 50ºC.The current used by the sensor is 22 mA at 12 volts, (Table 1).

ATmega 16 has an advanced RISC architecture with 32 general-purpose registers, 8-channel 10-bit Analog to Digital Converter (ADC), 32 programmable input/output (I/O) ports and work at 16 MHz; the ATmega16L microcontroller has an on chip oscillator, power on reset and programmable power failure detection. The voltage signals coming from the optical sensors are introduced to ATmega16 ports PA0-PA3, (Fig. 3).

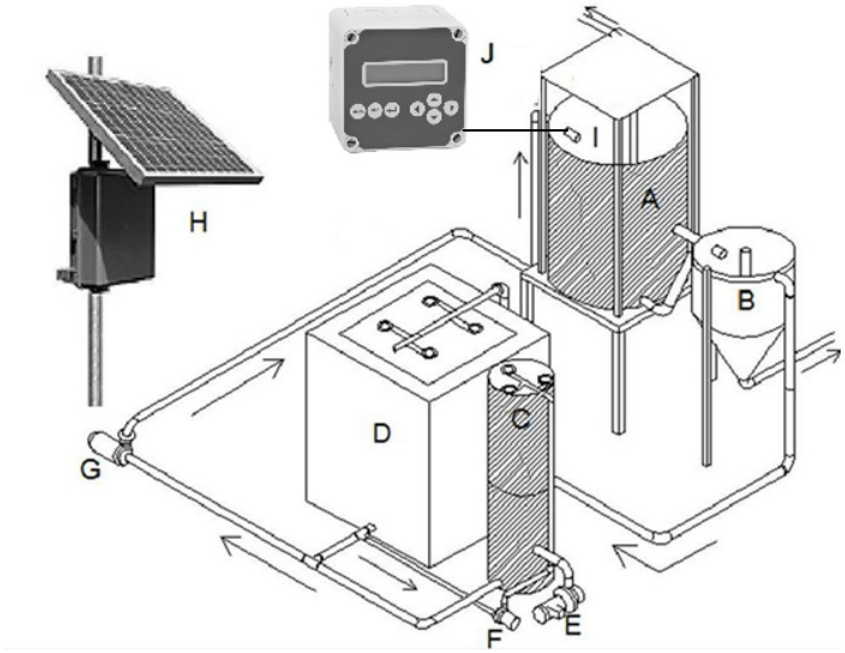

Fig. 1. View of a RAS system showing (a) culture tank, (b) separator, (c) column aerators, (d) bio-filter, (e) aerator fan, (f) aerator pump, (g) recirculating pump, (h) photovoltaic system, (i) DO sensor and (j) DO controller

Table 1. Power consumed by one RAS including the monitoring chamber

Location	Equipment	Operating hours	Power, W	Flow, L/m	Pressure, m	Voltage, V
RAS	Recirculating pump	20	90	41	2.5	120 AC
RAS	Aerator pump	20	90	30	6	120 AC
RAS	Aerator fan	20	373	400‡		120 AC
Controller	Air pump	0.1	12	9	21	12 DC
Controller	Sensor	24	1.05			12 DC
Controller	Controller	24	25			12 DC

‡ *air flow in* m^3/h

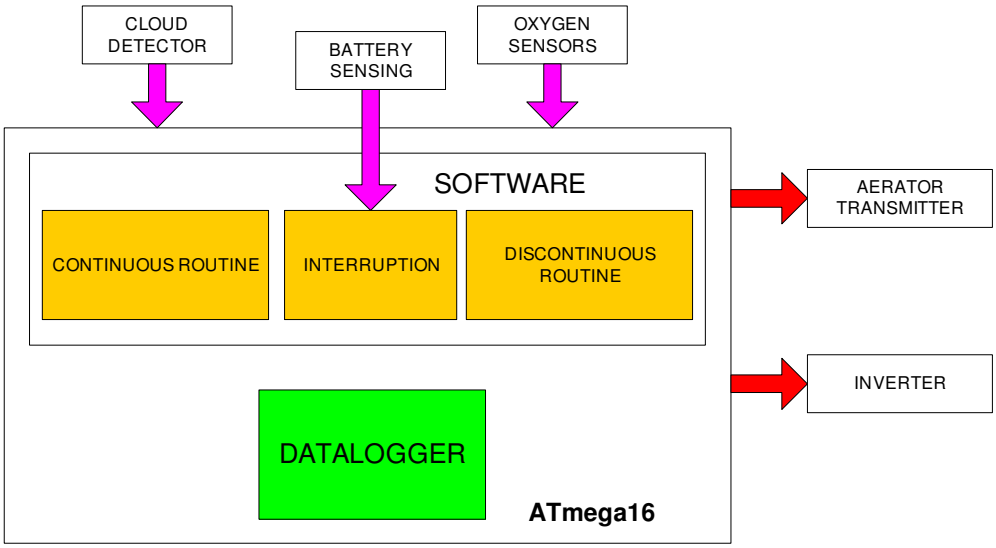

Fig. 2. Block diagram of the controller

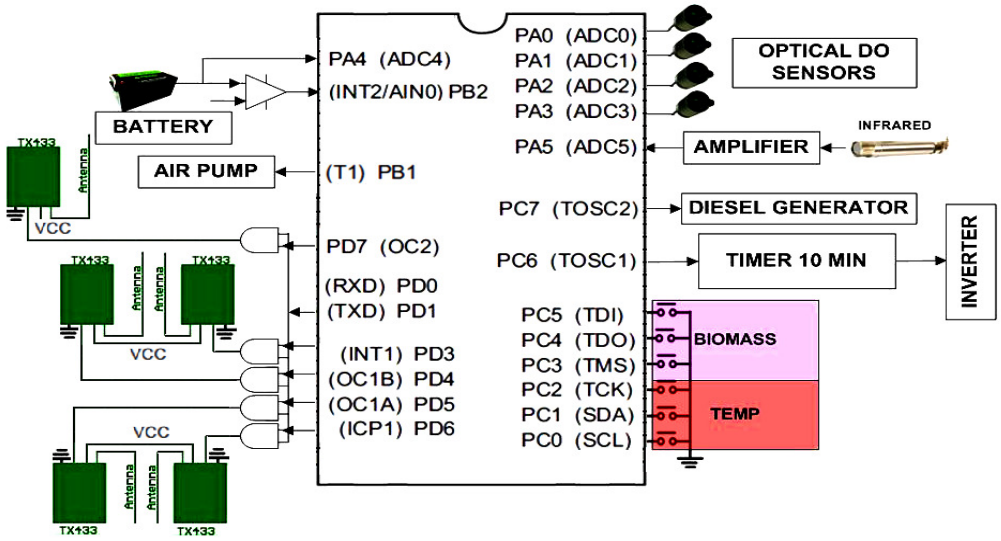

Fig. 3. A tmega16 pin description

Sensors are calibrated every week using air saturation value (6.4 ppm @ 20℃ @ 2400 m above sea level) as the first calibration point; for the second point a (zero oxygen) bisulphite solution was used. This calibration is done from the first week until fish harvesting. Before calibration the probe should be hydrated at least 24 hours, and requires at least 5 minutes for stabilization if the body temperature is different to room temperature. The probe presents a nozzle for the auto-clean by external pressure air. The Mini D2028 12VDCair pump of air was turned-on by a solid state switch activated by port PB1; the diaphragm pump provided 21 m of pressure @ 9 Lpm.

A detector sensitive to the presence of clouds was developed with an infrared thermopile in the 8-14 µm [17]. For this controller cloud presence was detected using an infrared non-contact transmitter (mod. OS301-LT-MV, Omega, USA). The 0-50 mV output was amplified by 10 and acquired by microcontroller port PA.5 and compared internally against a programmed threshold, (Fig. 3); the sensor measures from -20 to 100℃. Measurements were taken during two months to correlate clouds presence with sensor measurements. Battery voltage is multiplied by 0.36 and acquired by port A.4. The signal provided by the operational amplifier which compares the battery voltage against a threshold is fed to the external interruption pin (port PB.2).

DO provided by each sensor is acquired every ten-minute interval being sampled in a one minute basis; the value is averaged and stored in the microcontroller internal EEPROM memory. TheATmega16 has a 512 EEPROM memory and uses three memory locations to save each averaged DO value. The first data stores the sampling time, being the hour stored in the first nibble and the minute in the second nibble. The second and third data stores the entire and decimal part of the DO measurement, respectively. Four averaged DO measurements obtained from the sensor inside each tank are saved every ten minutes together with its sampling time during 6 hours. After this period, values are transmitted by means of a TX433 module to a storing device; during transmission, port PD.7 exits a five volt signal to an AND gate.

When the average dissolved oxygen value of the tank is beneath the DO set point, the aerator will be turned-on. This routine is repeated for each tank since each aerator is controlled independently. Four RF-TX-433 small transmitter modules were used to transmit signals to turn-on remotely (100 m) the aerator pump and fan. The modules supplied by a 3 V battery consumed 9 mA during operation and 20 mA during transmission at 433 MHz. Four digital signals from ports PD.3 to PD.6 were introduced to AND gates together with the transmit signal from port PD.1; the AND gate output fed one TX433 module, (Fig. 3).

2.4 Controller Software

The controller block diagram is explained in (Fig. 4. A). After setting each tank DO set-point, the embedded controller reads the temperature and biomass conditions set by the producer by activating the pins of a 6 bit DIP switch on a weekly basis. The first three bits connected to ports PC.3-PC.5 represented one of the eight biomass categories; the last three bits PC.0-PC.2 indicated to the water temperature ranging between 17 and 24℃.Once known the water temperature and the biomass density, a look up table provides the required aeration time per tank to maintain a 5 ppm DO (Table 2). For example for a biomass of 22 kg/m^3 @ 20℃, 15.17 hours are required. A time counter(TC) is used to indicate when the EEPROM memory is full and the data has to be transmitted; this counteris cleared at the beginning of the routine. The routine starts checking whether the day is cloudy and activates a timer turning the inverter for ten minutes.

The controller routine (Fig. 4.B) monitors the DO level in each of the four tanks taking one measurement per minute during all the day and night. The ten measurements are averaged and the mean value is saved in the ATmega16 EEPROM memory; this value is compared against the DO set-point. When the tank dissolved oxygen is lower than the desired DO, the aerator is turned-on for a 10 minute interval during continuous or discontinuous mode operation. During cloudy days, solar panels produce little energy and tanks are oxygenated based on the discontinuous routine (Fig. 4 A). Under discontinuous operation, the tank will be aerated for 60 minutes and 60 minutes no aeration will be applied.

When the battery voltage monitored by port PA.4 was beneath 11.7 Volts DC, an interrupting pulse was sent to PB.2 (Fig. 4. C); the diesel generator was turned-on through port PC.7. The oxygenation system was powered by the diesel

generator, and batteries were charged-up to 13 VDC. In this moment, the diesel generator was turned-off and the RAS system became powered by the photovoltaic system.

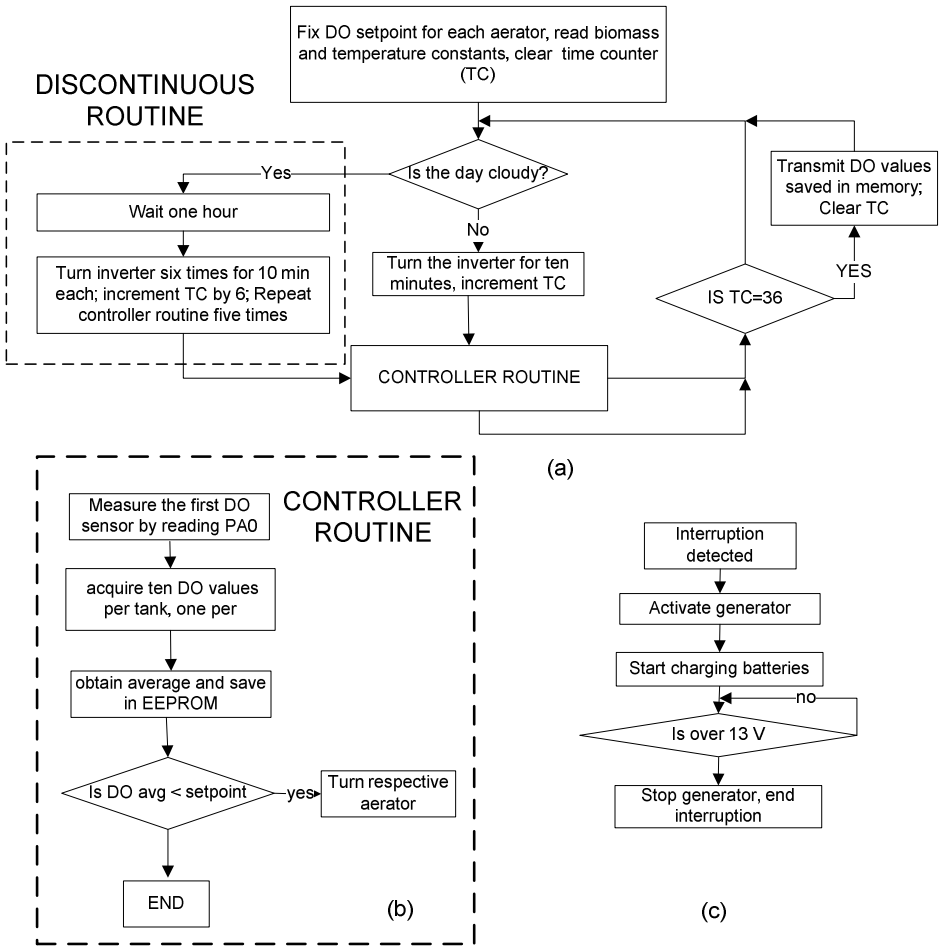

Fig. 4. Block diagram of (a) the entire process, (b) of the controller routine and (c) of the interruption routine

Table 2. Aeration required for different fish stocking densities (kg biomass) per cubic meter of water at different water temperatures to maintain DO of 5 ppm

Kg biomass per m^3 water	Aeration in hours for different water temperatures °C							
	17	18	19	20	21	22	23	24
2	1.83	1.94	2.12	2.25	2.38	2.51	2.63	2.76
6	5.00	5.30	5.77	6.11	6.51	6.90	7.20	7.60
10	7.68	8.16	8.85	9.33	10.00	10.64	11.06	11.73
14	9.87	10.52	11.36	11.92	12.85	13.75	14.21	15.15
18	11.56	12.38	13.30	13.86	15.06	16.22	16.65	17.85
22	12.75	13.75	14.68	15.17	16.63	18.04	18.39	19.85
24	13.15	14.25	15.15	15.58	17.18	18.72	18.99	20.58

3. RESULTS

Water was recirculated during the entire day in the aquaculture system and the controller turned-on the aerator fan and pump. The aerator motor and pump consumes 80% of the total energy. Open loop control based on aerator turn-on and turn-off intervals was programmed once the tank biomass was known. Closed loop control compared the sampled water dissolved oxygen with the DO set-point every ten minutes and turned-on the aerator.

3.1 Cloud Sensor

The cloud sensor based on the infrared sensor was installed at the end of April and started to operate on the first of May of 2011. The signal provided to the microcontroller was a 0-5 volt signal considering all the temperature range (-20℃-100℃); nevertheless measurements varied from 0.5 to 1.5 V. The signal was processed so that the values acquired by the ATmega 16 presented a better accuracy. The new circuit provided 5 V at 20℃ and 0V at -20℃. At the same time measurements were carried with a sunshine indicator (model SDE, THIES Clima, Germany) sensor which provides a 0-5 V output, corresponding to the global output radiation. Correlations between the radiation and the infrared sensor are shown in (Fig. 5).

Cloud cover appeared in 58% of the measurements between 15:00 to 16:00, (Fig 5 A); it was encountered in 80% of the measurements from 16:00 to 17:00, (Fig. 5 B).The green circle (Fig 5 A) shows values that cannot be successfully detected as clear or cloudy sky confusing the controller. For example, the sky of (Fig. 5 C) presents some clouds, but its radiation is 650 W/m^2 and the photovoltaic system generates energy; it is detected as cloudy and the system enters erroneously to the discontinuous mode routine. A dark sky (Fig. 5 D) limited sun radiation to 250 W/m^2 over the solar panel, being the cloud infrared voltage of 3.7 V. Infrared voltages acquired between 16:00 and 17:00 (Fig. 5 B) indicated the presence of clouds when the value was over 3.3 V; confusion occurred between 2.8 and 3.7 V. At measurements between 15:00 and 16:00 (Fig. 5 A) clouds were detected when the infrared value was over 2.8 V. Measurements indicated that an incident radiation of 350 W/m^2 can be available a 15:20 under cloudy sky or at 17:00 under bright sky; as well the threshold voltage for cloud detection is also hour-dependent.

Measurements were taken every ten minutes and interruption peakswere found when measurements drop below 2.2 V (yellow line); the peaks could last for several minutes. An interruption peak that lasted 4-ten minute periods (14:20 to 14:50) on May 16 presents a red circle marked as 12-15; blue circles indicate interruption peaks on May 2. A total of 6 interruptions were counted on May 2 and 12 in May 16 between 9:00 and 16:00 hours, (Table 3). In all the measurements recorded on the month of May no peaks appeared earlier than 13:00 hour, and most days between 16:00 and 17:00 presented 3 or more ten-minute periods with clouds and consequently very low irradiation, (Table 3).

Some days present sunny and cloudy intervals, (Fig. 6). The sunshine indicator used as an alternative to the cloud sensor showed several peaks on May 2 and May 16, (Fig. 6).

3.2 Radiation Conditions and PV System Performance

Environmental conditions can have a significant impact on the efficiency and proper operation of a photovoltaic system. Cloud cover in all the regions of Mexico was reported in the year 2002 in a monthly basis [18]. February had only 12 days with clouds in the region of Texcoco, Mexico; July, June and May presented 30, 27 and 26 cloudy days, respectively. Daily solar radiation was classified as poor (<220,000 kW/m^2), medium or high (over 250,000kW/m^2). In May, six days presented high radiation, and ten day were completely cloudy (poor radiation). In the month of June, nine days were poorly radiated, and twelve presented strong radiations (all day sunny). Solar radiation reached 500 W/m^2 at a different time every day, being between 08:30 and 08:40, (Table 3); May 3 started at ten o´clock in the morning and presented the lowest radiation of the month although it presented 30 minutes over 1000 W/m^2. Three or more irradiation hours over 1000 W/m^2 per day were present in only 19% of the days in May; 45% of the days in May had less than 2 hours of irradiation over 1000 W/m^2. The number of hours with irradiation over 1000 W/m^{2}during seven randomly selected days are shown in (Table 3). Daily irradiation decreased with cloud cover which is correlated to the number of interruption peaks.

The current stored in the batteries and the current produced by the solar panels were data-

logged every second. Daily radiation varied between 150,000 and 260,000 kW/m^2. When the energy produced by the solar panels was greater than the energy used by the recirculating system, the exceeding energy was saved in batteries (10:00-16:15) during May 23, (Fig. 7); from 16:30 on, the energy consumed by the system was only provided by the battery. The energy stored by the battery at 20:00 was 62 Ah on May 23; it was only of 25 Ah on May 3. The regulator limits battery overvoltage over 14 V and avoids excessive deep discharges that could damage the battery.

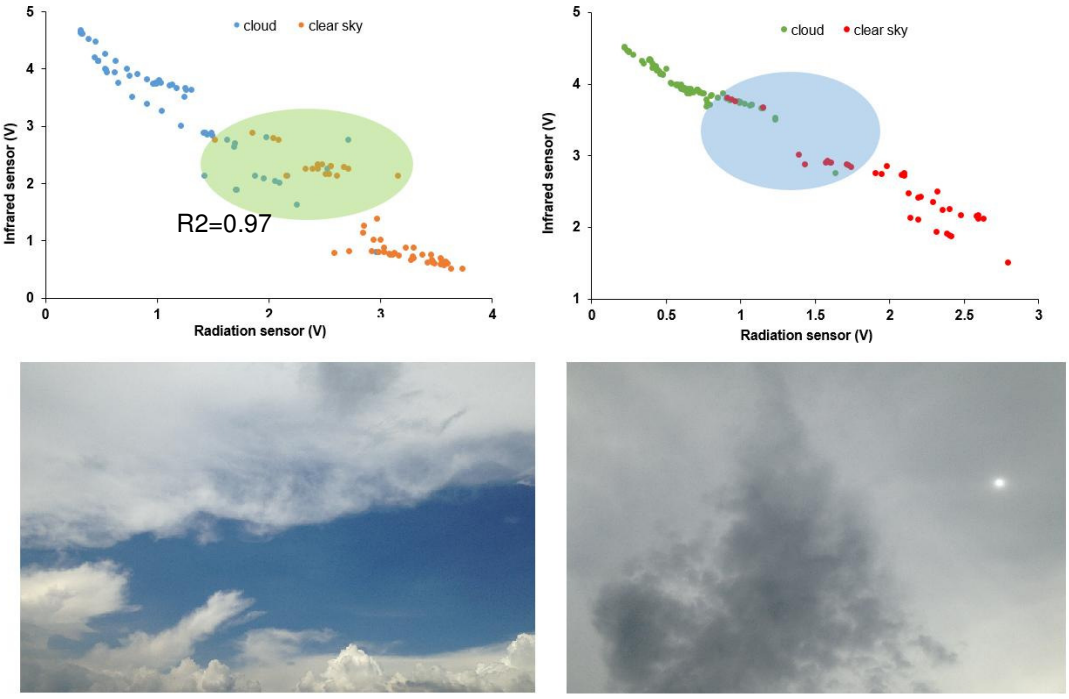

Fig. 5. Radiation and infrared sensor measurements taken (a) between 15:00 and 16:00 hours, (b) 16:00 and 17:00 hours, (c) sky image with a mixture of clouds and clear sky, and (d) image of a dark cloudy sky

Table 3. Time when radiation overpass 500W/m^2, daily hours having 1000 W/m^2, daily radiation, current produced by panels and quantity of cloud detection intervals

Day	Radiation over 500 W/m^2 starts at	Radiation hours over 1000 W/m^2	*Daily radiation, KW/m^2	TSolar panels prod, A/day	Clouds interrupt 9:00-16:00	Clouds interrupt 16:00-17:00
May 2	08:50	3:20	238,650	128.6	6	4
May 3	10:00	0:30	162,174	87.4	25	5
May 8	08:30	2:50	257,556	138.8	1	4
May 13	08:50	2:50	252,369	136	0	3
May 16	08:50	2:00	212,907	114.7	12	5
May 21	08:30	1:40	210,765	113.6	13	3
May 23	08:30	1:30	249,711	134.6	3	4

**Measurements taken every second; TMeasurements taken every second*

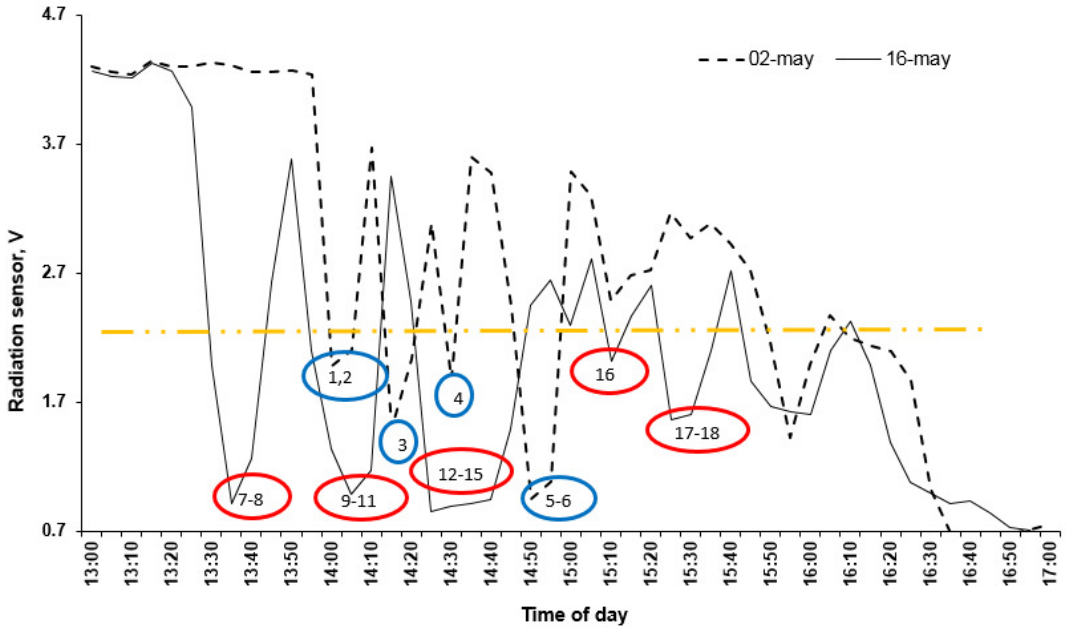

Fig. 6. Interruptions detected by the radiation sensor on May 2 and May 16

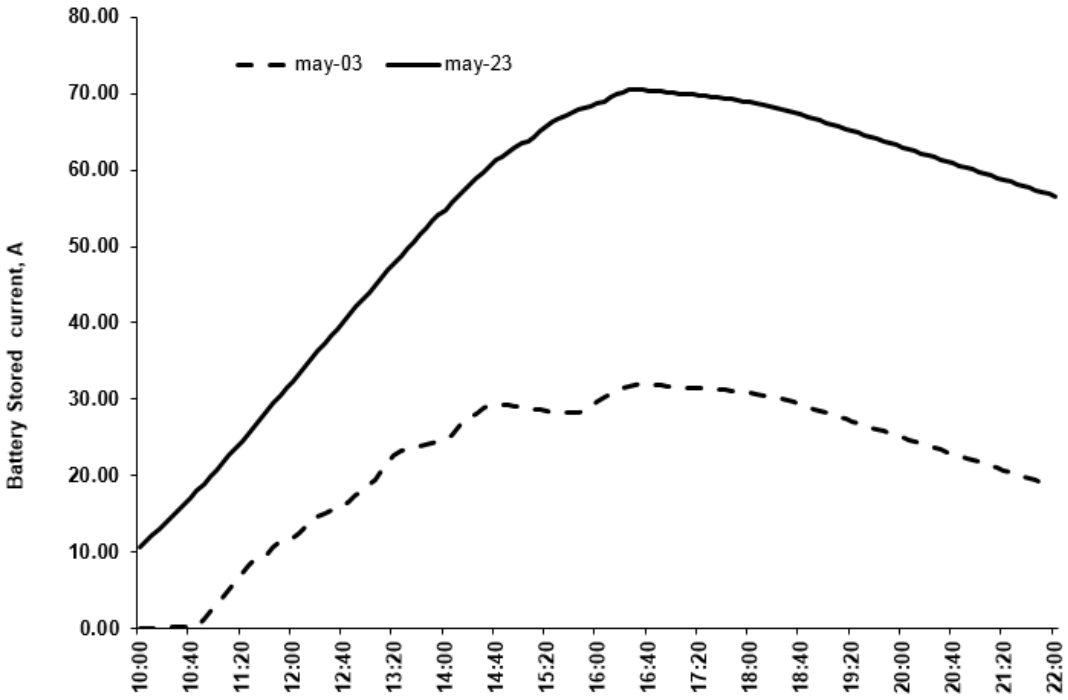

Fig. 7. Interruptions detected by the radiation sensor on May 2 and May 16

When the irradiated solar energy became lower than 200 W/m^2, the system was unable to provide the current required by the system. On May 3, severe clouds reduced radiation income to solar panels beneath 450 W/m^{2}in the periods: 11:35-12:00; 13:30-13:55; 14:25-15:50 and

16:20-on. According to block diagram (Fig. 4 A) once a cloudy moment is detected, the discontinuous routine (DR) starts operating and lasts 2 hours before another process takes place. The DR routine started working at 11:35 until 13:35 and at 13:40 another cloudy measurement was detected re-starting the DR routine again until 15:40; the controller continued with DR routines until 19:50. The current available at the battery after charging all day on May 3 using the continuous routine was of28.24 Ah@ 19:00 (Fig. 7), meanwhile with the discontinuous routine it was 44. 13 A. A battery with a charge of 39 Ah at 19:00can provide continuous energy during all the night; with 28.24 Ah @ 19:00, the aerators stopped working at 3:45. On May 23, after continuous aerator operation during all day and night, 30.8 Ah were still present at 7:00 next morning. At the end of cloudy days without sunshine the accumulated current in the battery ranged from 39 to 49A depending on the radiation throughout the day; a high standard deviation of 8.73 was obtained.

After monitoring daily the battery voltage at 7:00 in the morning on May, the voltage varied between 12.3 and 14 V, (Fig. 8). May 3 was the most critical day of the month with a total collected radiation of 162174 kW/m^2. Voltage in this day felt from 13.8 to 12.9V, but increased to 13.3 V on May 13. Afterwards, the voltage felt again to 12.2 V, recovering to 14 V on May 29.

3.3 Controller Performance

Transmission of signals between the TX-433 module and the RX-433 reception module placed at the aerator control box, worked properly. Rainy days, fog and morning's high relative humidity did not caused problems during transmission. The data logger saved DO data every 6 hours but its program was modified in order to save also solar radiation values; another two bytes were used for storing each value getting the memory full after 3 hours.

Biomass and temperature were changed in order to check whether the number of aerated hours took place. Decimal values of the aeration hours required on (Table 2) increased program size so they were truncated to the nearest entire number; using the truncated did not reduce fish growth. Fish growth pattern and its correlation with DO consumed is clearly explained by El Messery [19]. After plotting DO versus time for a biomass of 25 kg m^{-3}, the time constant was found to be 90 minutes. When the aerator stopped for 40 minutes, in a tank having a biomass of 25 kg m^{-3},dissolved oxygen decreased from 5 to 3.2 ppm. When the aerator stopped by 30 minutes DO decreased from 5 to 3.65 ppm. If the aerator turned-off one hour, DO decreased from 5 to 3 ppm for a biomass of 14 kg m^{-3}.

If the discontinuous routine worked all night, DO decreased from 4.8 to 4.4 ppm in the tank but consumed 17% less energy, (Table 4). It is important to note that DO values at 7:00 in (Table 4) correspond to DO concentrations of the next day. For example, in the half cloudy day (third row) with night discontinuous oxygen feeding and the starting DO concentration of 4.8 ppm in the morning decreased to 4.7 ppm at 19:00. After all night having discontinuous control, DO felt to 4.2 ppm at 7:00 ppm.

After several discontinuous periods of one hour, dissolved oxygen concentration decreases and never recovers its initial value. For example, DO @ 14:00 was 4.54 ppm, and after two hours the maximum value recorded was 4.29 ppm. Discontinuous periods of one hour cause stress in fish as DO oxygen decreases below 2.5 ppm, (Fig. 8). DO in the tank minimum values of 3.24 and 4.16 ppm were encountered for 30 and 10 minute discontinuous periods, respectively. As the three treatments save the same amount of energy, the ten minute discontinuous routine results the best as DO remains over 4.1 ppm.

Table 4. DO values at 7.00 and 19:00 for a biomass of 20 kg per m^3 of water and energy saved by each of the three control using a DR period of one hour

Treatment	Dissolved oxygen, ppm		Energy consumption, Ah	
	At 7:00*	At 19:00	Day	Night
All day	4.8	4.8	64	64
Al night DR	4.4	4.8	64	53.16
Half day all night DR	4.2	4.7	58.58	53.16
All day DR	4.1	4.1	53.16	53.16

**Next day measurement*

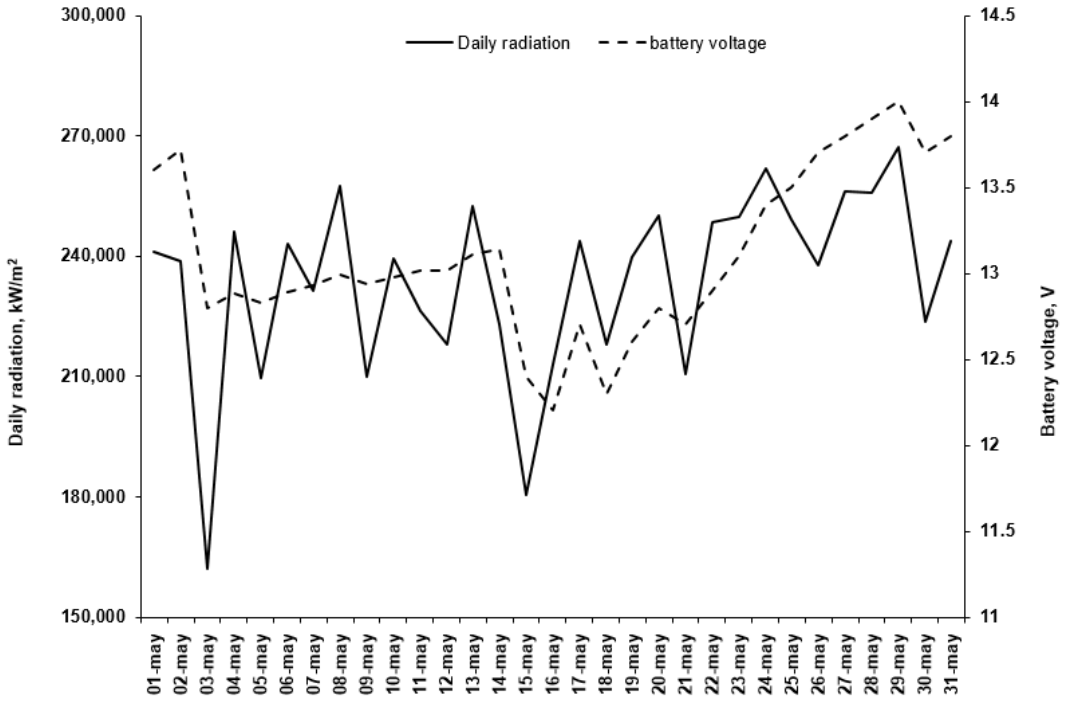

Fig. 8. Daily battery voltage at 7:00 and daily total radiation

4. DISCUSSION

Clouds impact and its spatial distribution is a key component in the global climate and its understanding can contribute to improve weather predictions. Spatial cloud distribution can help to model their effect in energy production on photovoltaic systems. Several zenith-viewing active sensors are being used to provide a more complete diurnal cloud coverage as the Micro-Pulse Lidar and the wave cloud radar [20]. Infrared thermometry in the 8-14 µm band is used to detect the presence and temperature of clouds for meteorological research [21-23]. Water vapour correction in an infrared cloud imager measured -40°C for clear sky and 0°C for cloudy sky [20]. A similar Omega OS540 IR sensor to the one used in this development, measured precipitable water in the South of Texas; temperatures ranged from 2 to 35°C [22].

The OS301-LT-MVsensor used by the controller measured correctly the presence of clouds, but was not selective for detecting slight (400-600W/m^2), moderate (200-400 W/m^2) or heavy clouds (lower than 200 W/m^2). When the IR sensor is directed to the zenith it does not follow the sun movement, so the measurement is not always true. It is better to obtain a direct radiation measurement using a cheap PAR sensor [24] or use the sunshine indicator placed by the side of the solar panel having the same inclination; it detects exactly the radiation received by the photovoltaic system.

Clouds move with air and after short periods of time, the sun will appear between the clouds and shine, so the IR sensor will measure a clear sky. High frequency sampling should be made and the algorithm should take into account previous measurements. Once the discontinuous routine starts, it cannot be changed until two hours later; sky measurements should be obtained continuously to train an intelligent model-decision system. Fourier together with wavelet algorithms have been used to provide a smoothing effect, which reduced short-term fluctuations due to weather changes [25]. Spikes are generated by fast passing clouds which can be smoothed, meanwhile perennial clouds will cause irradiation drops; slow moving clouds present very small irradiance variations.

As high irradiation hours (over 1000 W/m^2) in Texcoco are limited between 1.5 and 3 hours, optimization on the utilization of solar energy depends on solar power management technologies. A power converter for maximal power point tracking (MPPT) is inserted between

the solar cell panel and the load to control power flow [26]. Battery charging is of concern in order to optimize its use in photovoltaic systems [27]. In this application a simple protection charger was used, protecting the batteries against overvoltage and also avoiding a high depth of discharge (DOD) which will reduce battery lifetime; depth of discharge was limited to 70% and when the voltage was that low, the discontinuous routine was activated. Current charge and discharge were also limited to protect the batteries.

Many MPP tracking (MPPT) methods have been developed varying in complexity, sensors required, convergence speed, cost, and range of effectiveness [28]. Another slave microcontroller could be used as a MPPT power converter and the tracking system has to automatically find the voltage or current at which a PV array will operate to obtain the maximum power output under a given temperature and irradiance. The information gathered during the last two years of solar irradiation, temperature, PV panel current, PV voltage should be employed to develop an intelligent power converter [26,29]. If the battery current during charging is maintained at a constant high level, the battery voltage increases fast until it reaches the gassing voltage (Vg=2.35V) in lead batteries [30]. During battery charging, the internal resistor still depends on battery state of charge (SOC); its value increases at a high rate when battery SOC is high [30].

DO sensors worked properly and required little maintenance and calibration and the controller acquired and data-logged the data; it also turned-on the aerators remotely. The control program was evaluated searching for energy efficiency and DO optimum concentration. Three requirements have to be addressed: how many hours should the aerators be turned-on in the night, effective cloud sampling and optimum period for the discontinuous routine. The aerators should be turned-on using a ten-minute discontinuous routine (Fig. 9) during all the night optimizing energy, (Table 4). Cloud cover should be sampled every minute; its analysis should consider the average of the last twenty measurements and a derivative to take the proper corrective action.

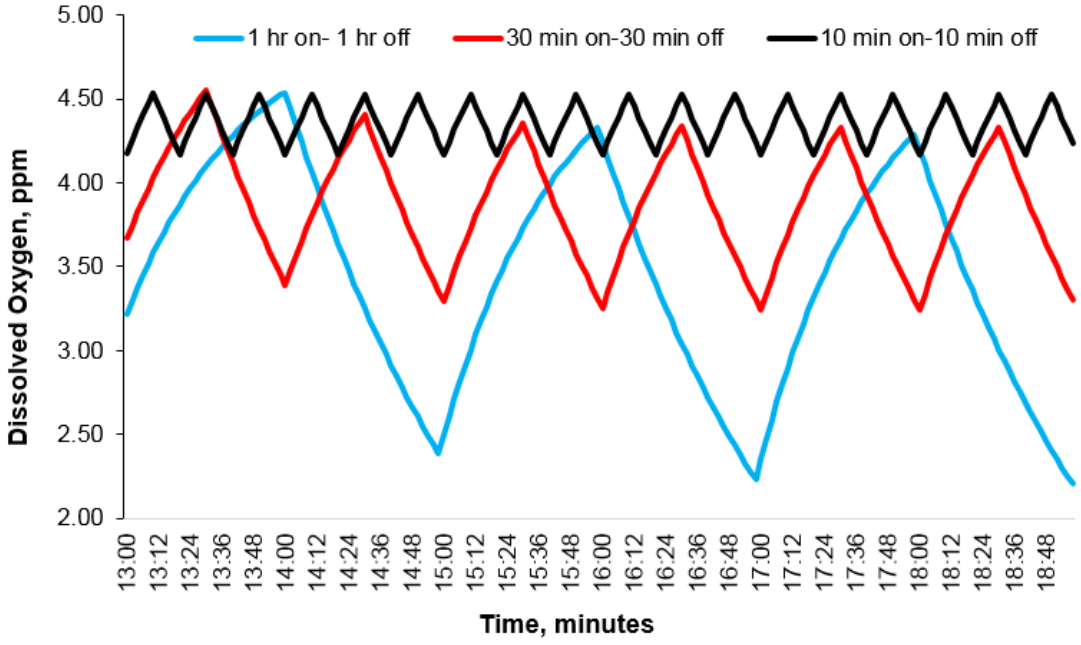

Fig. 9. Effect on water tank dissolved oxygen caused by different discontinuous routine periods

Fish move less during the night but continue breathing, and consumes more oxygen when it moves. For example, cod swimming at maximum speed (57 ms^{-1}) in the Atlantic presented a 65% increase in DO consumption with respect to the fish at rest [31]; cod heart beat presented peaks between 7:00 and 19:00 hours and a steady operation in the night. Using the DO-heart beat correlation, a reduction of 76% in DO consumption appears in the night. In trout aquaculture in ponds, LDO was monitored with HACH LANGE LDO sensors, and when it felt below 10 mgl^{-1}, a drum aerator was activated. It was noted that water ponds presented LDO values beneath 10 ppm between 6:00 and 13:00 and between 17:00 and 22:00 [32]; values between 00:20 and 6:00 presented values ranging between 11 and 13 ppm LDO.DO demand in carp tanks varied from 4-5 ppm between 11:30 and 4:00 [33], compared to 5-6 during daytime. Based on these studies and considering a 50% less DO consumption, the discontinuous routine could be used during the night saving a lot of energy. (Table 2) can be considered as a base look-up table where depending on the biomass and the temperature, the number of oxygenation hours are known for growing fish. In a closed loop system aerator turn-on is given by DO measurement, non-dependent on fish variety. During cloudy periods, energy management is fundamental for PV system sizing, but studies on fish growth should be done; several varieties should be studied as well as fish growth under reduced oxygenation periods.

5. CONCLUSION

This paper shows that only 19% of the days on May presented 3 hours of 1000 W/m^2, so the controller managed energy efficiently. The controller hardware acquired the signals properly, data-logged DO average values and transmitted the pulses remotely to turn-on the aerators. The cloud sensor was correlated against a radiation sensor and the latter was finally used; confusion exists when rapid moving clouds are present in the sky. Radiation measurements are hour-dependent so the ATmega 16 real time clock was synchronized with the cloud acquisition routine. A MPPT tracker would optimize battery charging and energy management in the photovoltaic system.

Energy optimization management has to consider water tank DO stable concentration, so the critical tunings of the software controller were defined. These requirements included water DO under different discontinuous routine intervals. Energy savings of 17% were encountered, when the DR was used throughout the night; DO concentration did not decrease below 4.1 ppm using ten minute intervals. The effect of sudden cloud peaks was reduced with averaging and by using derivatives to determine changes in the cloud cover; its sampling frequency was increased from 10 minutes to 1 minute. When the system operates during all the night under discontinuous periods, fish growth is not affected.

COMPETING INTERESTS

Authors declare that there are no competing interests.

REFERENCES

1. Applebaum S, Parilutsky A, Birkan V. An emergency aeration system for use in aquaculture. Aquacultural Engineering. 1999;20:17-20.
2. Butler B, Burrows DW. Dissolved oxygen guidelines for freshwater habitats of Northern Australia, ACTFR Report No. 07/32. Australian Centre for Tropical Freshwater; 2007.
3. Masser M, Rakocy J, Losordo TM. Recirculating aquaculture tank production systems. SRAC Publication No. 451. Southern Regional Aquaculture Center. USDA; 1992.
4. Appiah-Kubi F. An Economic analysis of the use of recirculating aquaculture systems in the production of Tilapia. MSc Thesis, Department of Animal and Aquaculture Sciences, Norwegian University of Life Sciences, Ås, Norway; 2012.
5. Boyd CE, Tucker C, McNevin A, Bostick K, Clay J. Indicators of resource use efficiency and environmental performance in fish and crustacean culture. Reviews in Fisheries Science. 2007;15:327-360.
6. Boyd CE. Pond water aeration systems. Aquaculture Engineering. 1998;18(1):9-40.
7. Appelbaum J, Mozes D, Steiner A, Segal I, Bark M, Reuss M, Roth P. Aeration of fish-ponds by photovoltaic power. Progress in Photovoltaics. 2001;9:295-301.
8. Mohamad NR, Soh AS, Salleh A, Hashim NMZ, AbdAziz MZA, Sarimin N, Othman A, Ghani ZA. Development of aquaponic system using solar powered control pump.

IOSR Journal of Electrical and Electronics Engineering (IOSR-JEEE). 2013;8(6):1-6.

9. El Nemr MK, El Nemr MK. Fish farm management and microcontroller based aeration control system. Agric Eng Int. CIGR Journal. 2013;15(1):87-99.
10. Simbeye DS, Yang SF. Water quality monitoring and control for aquaculture based on wireless sensor networks. Journal of networks. 2014:9(4):840-849.
11. Lu Z, Piedrahita RH, Neto CD. Generation of daily and hourly solar radiation values for modeling water quality in aquaculture ponds. Transactions of the ASAE. 1998;41(6):1853–1859.
12. Wong LT, Chow WK. Solar radiation model. Applied Energy. 2001;69:191–224.
13. Choi YK. A study on power generation analysis of floating PV system considering environmental impact. International Journal of Software Engineering and Its Applications. 2014;8(1):75-84.
14. Guodong Y, Shuying L, Jisheng L, Yong H, Shangwen C. Effect of wind-solar complementary increasing oxygen system in aquaculture. Advance Journal of Food Science and Technology. 2013;5(12):1652-1659.
15. Hahn F. Self-powered instrumentation equipment and machinery using solar panels, In: Ochieng, R.M. (ed.) solar collectors and panels, Theory and Applications. Sciyo International, Vienna, Austria. 2010;293-314.
16. Jayakumar P. Resource assessment handbook. Asia and Pacific Center for Transfer of Technology (APCTT); 2009.
17. Clay RW, Wild NR, Bird DJ, Dawson BR, Johnston M, Patrick R, Sewell A. A cloud monitoring system for remote sites. Publications Astronomical Society Australia. 1998;15:332-335.
18. Becerril MA. Historical analysis of the climate in Mexico. Thesis degree in Hydraulic Engineering. Universidad Autonoma Metropolitana; 2003.
19. Elmessery WM. Design of automatic food dosing and oxygenation for a carp recirculating aquaculture system. PhD Dissertation. Chapingo University, Mexico; 2011.
20. Thurairajah B, Shaw JA. Cloud statistics measured with the infrared cloud imager (ICI). IEEE Transactions on Geo Science and Remote Sensing. 2005;43(9):2000-2007.
21. Morris VR, Long CN, Nelson D. Deployment of an infrared thermometer network at the atmospheric radiation measurement program Southern Great Plains Climate Research Facility. Sixteenth ARM Science Team Meeting Proceedings, Albuquerque, NM; 2006.
22. Mims FM, Chambers LH, Brooks DR. Measuring total column water vapor by pointing an infrared thermometer at the sky. Bulletin American Meteorological Society. 2011;92:1311–1320.
23. Maghrabi A, Clay R, Wild N, Dawson B. Design and development of a simple infrared monitor for cloud detection. Energy Conversion and Management. 2009;50(11):2732-2737.
24. Lorenzo E. Energy collected and delivered by PV modules, in Handbook of Photovoltaic Science and Engineering (eds A. Luque and S. Hegedus), John Wiley & Sons, Ltd, Chichester, UK; 2005.
25. Kawasaki N, Oozeki T, Otani K, Kurokawa K. An evaluation method of the fluctuation characteristics of photovoltaic systems by using frequency analysis. Solar Energy Materials and Solar Cells. 2006;90(18–19):3356-3363.
26. Takun P, Kaitwanidvilai S, Jettanasen C. Maximum power point tracking using fuzzy logic control for photovoltaic systems. Proceedings of the International Muti Conference of Engineers and Computer Scientists. 2011;2. IMECS 2011, March 16-18, Hong Kong.
27. Sree B, Ramaprabha R, Mathur BL. Design and modelling of standalone solar photovoltaic charging system. International Journal of Computer Applications. 2011;18(2):41-45.
28. Esram T, Chapman PL. Comparison of photovoltaic array maximum power point tracking techniques. IEEE Transactions on Energy Conversion. 2007;22(2):439-449.
29. Wilamowski BM, Li X. Fuzzy system based maximum power point tracking for PV system," Proceedings 28th Annual. Conference IEEE Industrial Electronics Society. 2002;3280–3284.
30. Fakham H, Lu D, François B. Power control design of a battery charger in a hybrid active PV generator for load-following applications. IEEE Transaction

on Industrial Electronics. 2011;58(1):85-94.

31. Claireaux G, Webber DM, Kerr SR, Boutilier RG. Physiology and behavior of free swimming Atlantic cod (*Gadus morhua*) facing fluctuating salinity and oxygenation conditions. The Journal of Experimental Biology. 1995;198:61-69.

32. Tautenhahn A, Karg U. Process analysis LDO optical oxygen probe trout farming. Application report No. 043.52.00490 2007.

33. Elmessery WM, Abdallah SE. Intelligent dissolved oxygen control system for intensive carp system. New Ground Research Journal of Agricultural Science and Technology. 2014;2(1):33-45.

Peer-review history:
The peer review history for this paper can be accessed here:
http://www.sciencedomain.org/review-history.php?iid=713&id=5&aid=6579